Analysis of Energy Storage Operation Configuration of Power System Based on Multi-Objective Optimization

Linyao Zhou*, Tengfei Ma

Xi'an Jiaotong University City College, Xi'an 710018, Shaanxi Province, China

*Corresponding author: Linyao Zhou, zhoulinyao916@outlook.com

Abstract: Driven by the goal of "carbon neutrality," the increase in use of renewable energy power systems will be inevitable in the future. Uncontrolled output power and random volatility make it difficult to balance power in real time during system operation. Therefore, energy storage is considered to be an effective way to ensure the real-time balance of system power. However, cost of energy storage is relatively expensive. As a solution, energy storage can be used to balance the system power in order to reduce system operating costs. Taking the high proportion of wind power systems as an example, the impact of the "supply side" low-carbon transformation on the economics and reliability of power system operation is explored. In order to solve the problem of power system operation configuration optimization under the background of "carbon neutrality," this paper establishes a multi-objective programming model.

Keywords: Multi-objective planning; Energy storage analysis; Carbon-neutral; Carbon neutrality; Multi-objective programming model

1. Background and elaboration of the problem
1.1. Background of the problem

Carbon neutrality in power systems can be achieved by using renewable energy power systems. The strong random fluctuation of renewable energy output power makes it difficult to balance power in real time during system operation. Energy storage is considered to be an effective method to ensure the real-time balance of system power, because the cost of energy storage is relatively expensive, the use of energy storage balance system power will decrease the cost of system operation. Wind power systems were used as examples to study the impact of the "supply side" low-carbon transformation on the economics and reliability of power system operation.

The system that was studied includes thermal power, wind power, energy storage and load, 3 thermal power units, and an installed capacity of 1050MW. On a given day, the wind power and load normalization power (1.0 p.u. wind power corresponds to its installed capacity, and 1.0 p.u. load corresponds to the maximum load power) data are shown in the **Appendix 1**, the increase in wind power penetration (the ratio of maximum wind power to maximum load power) may cause system wind abandonment and load loss, affecting the system power balance.

Definition: System unit power supply cost = (total cost of system power generation) / (total load of the system), total cost of power generation = (thermal power cost) + (wind power cost) + (energy storage cost) + (curtailment loss) + (lost load loss).

The cost of thermal power includes operating costs and carbon capture integration costs, of which the operating costs of thermal power are determined by the operation and maintenance costs and the coal consumption costs of power generation composition, the relationship between coal consumption, and its output: $F = aP^2 + Bp + c$, where F is the coal consumption of the unit (kg/h), and P is the output of the unit/MW; The operation and maintenance cost is considered according to the cost of 0.5 times coal consumption, whereas carbon capture integration depends on carbon emissions and carbon capture unit price. The relevant parameters of thermal power units are shown in **Appendix 1**, and the price of thermal coal is 700 yuan/t. Wind power costs only take into account the cost of operation and maintenance, and the relevant parameters are as shown in **Table 2**. The cost of energy storage consists of investment costs and operation and maintenance costs, and the relevant parameters are as shown in **Appendix 3**. Note: When calculating the cost per day, the investment cost needs to be amortized to each day, that is, the average daily investment cost = total investment cost / operating life / 365 days. Curtailment losses are calculated at 0.3 yuan/kWh and load losses are calculated as 8 yuan/kWh.

1.2. Elaboration of the problem

(1) Problem 1

Without wind power access, thermal power operates at minimum cost. A daily power generation plan curve of the unit was constructed. Then, the unit power supply cost of the system was calculated, and the values were recorded in **Table 1**.

(2) Problem 2

When the wind power installed capacity is 300MW with unit 3 as the replacement unit, what changes occurs in the power balance of the system? In this scenario, in order to reduce the curtailment without losing the load, how much can the installed capacity of wind power access be reduced?

(3) Problem 3

When the wind power is installed at 600MW and with 2 replacement units, what changes in the power balance of the system? In this scenario, how much can the wind power access capacity be increased in order to not lose the load?

(4) Problem 4

Based on the scenarios mentioned in (2) and (3), considering the aforementioned four carbon capture costs, the system supplies power according to the lowest power generation cost. Then, the unit power supply cost of the system was calculated, and relevant calculation results are shown in **Tables 2 and 3**.

(5) Problem 5

When the wind power is installed at 900MW and the replacement unit is 2 or 3, how much power is lost? What is the minimum energy storage capacity that needs to be configured (90% charge-discharge efficiency) to keep the load out? Considering the cost of energy storage and the cost of capturing carbon per unit (60 yuan/t), what will be unit power supply cost of the system?

(6) Problem 6

When the load power is unchanged, what challenges does the increasing replacement capacity of wind power bring to the reliability of power supply of the system? What would the cost per unit of power supply of the system be like in order to ensure reliable power supply? Quantitative analysis was carried out in conjunction with the corresponding calculations.

(7) Problem 7

For the fifteen-day load power (maximum 1200 MW), wind power (installed capacity) shown in **Appendix 2** (1200 MW capacity), with thermal units 2 and 3 replaced with wind power units, what are the problems in the system power balance? A possible solution was designed in order to achieve power balance, and the feasibility and effectiveness of the solution were discussed.

2. Solution

2.1. Analysis of Problem 1

For Problem 1, In order to determine the minimum cost of the daily power generation plan curve, the load power was first adjusted to 900WM to obtain the load demand, and then the same method was used for each unit to obtain the unit output at each moment. The possible combinations were then listed, which correspond to each time period, either a single unit or multiple units together. Based on the list, the corresponding unit output were calculated, followed by the calculation of the corresponding coal consumption to further derive the cost. After summing up the calculated values, the combination that meets the load demand of the corresponding time period was determined. Then, the cost of each combination was compared, the minimum cost corresponding to the combination is the planned unit of the corresponding time period was determined, and the daily power generation plan was obtained by circulating 96 times. Once the plan is drawn, you can bring in the formula to derive the various costs in **Table 1**.

2.2. Analysis of Problems 2, 3, and 4

In Problem 2, thermal power unit 3 was replaced with a wind power unit. In order to explore the premise of reducing the curtailment of wind without losing the load, the appropriate extent of reduction of the installed capacity of wind power was first calculated. Then the 300WM of the wind power installed capacity was transversed with the step length set to 1. Next, the corresponding wind power technology outputs in different installed conditions were determined and was added to the thermal power unit 1 and 2. The total technical output of each period was determined. The total technical output is then diminished from the maximum load power of 900, the difference is greater than 0 for the wind curtailment, and less than 0 is the load loss; the sum of the values of the curtailed wind and the load loss were then calculated, and the minimum value of the of the calculated value was determined to obtain the optimal installed capacity and the associated curtailed wind power.

In Problem 3, under the premise of replacing unit 2, the calculation method is the same as Problem 2. As for Problem 4, parameters such as carbon capture on the basis of the calculation results of the first two questions were calculated.

2.3. Analysis of Problems 5, 6

(1) Problem 5

When the wind power is installed at 900MW and the replacement unit is 2 or 3, how much power is lost? What is the minimum energy storage capacity to be configured (90% charge-discharge efficiency) to be configured to keep the load out? Considering the cost of energy storage and the cost of capturing carbon per unit (take 60 yuan/t), what is the unit power supply cost of the system at this time?

(2) Problem 6

When the load power is unchanged, what challenges does the increasing replacement capacity of wind power bring to the reliable power supply of the system? What happens to the cost per unit of power supply in the system to ensure reliable power supply? Quantitative analysis is carried out in conjunction with the above calculations.

2.4. Analysis of Problem 7

For the fifteen-day load power (maximum 1200MW) and wind power (installed capacity 1200MW) shown in **Appendix 2**, under the scenario of wind power replacement thermal power unit 2 and 3, a possible power balance solution was designed, and the feasibility and effectiveness of the scheme will be discussed in the later part of this paper.

3. Model assumptions

In order to ensure the accuracy and ease of operation of the model, the interference of some insignificant factors was ignored, and several reasonable assumptions were made based on the actual situation.

(1) Hypothesis 1: Assume that the title data is true and valid.
(2) Hypothesis 2: It is assumed that the maximum technical output of each type of generator set can operate stably.
(3) Hypothesis 3: The engine keeps running well during operation.

4. Symbol description

$C1$: The investment cost of energy storage

P : Load

F : Total consumption coefficient

Out : The unit output

B_j : Installed capacity of fans

f_{ic} : Grid frequency

d_i : Annual discount rate for energy storage

5. Model building and solving

Based on the analysis of the aforementioned problems, a mathematical model was built and the process of establishment was explained, and the mathematical model was used to solve the issues.

5.1. Problem 1:

The investment cost and operating cost required to calculate the unit power supply cost of the system.

5.1.1. The investment cost of energy storage.

$$C1 = \frac{d(1+d)^L}{(1+d)^L - 1}(C^P P^{ESS} + C^e E^{ESS}) \tag{1}$$

Based on the equation, C1 represents the investment cost of energy storage, d is the annual discount rate of energy storage, L is the service life of energy storage; C^p and C^e represent investment costs per unit of power and unit capacity for energy storage, respectively; P^{ESS} and E^{ESS} indicate the rated power and rated capacity of the energy storage, respectively.

5.1.2. The operating costs of energy storage.

$$C_2 = C_{cha}P_{cha.t} - C_{dis}P_{dis.t} \tag{2}$$

C_2 represents the operating cost of energy storage; C_{cha} and C_{dis} represent the charging cost coefficient and discharge revenue coefficient of energy storage, respectively; $P_{cha.t}$ and $P_{dis.t}$ represent the charging and discharging power of the energy storage in the t-period, respectively.

Thermal power operates at the lowest cost, the daily power generation plan curve of the unit was generated, the unit power supply cost of the system was calculated, and the values are recorded in **Table 1** (retaining three significant digits).

5.1.3. Load conversion

First, the load power was converted into the desired value as shown below:

(1) Convert the load power into load output P_base

$$P_{base_i} = 0 + X_i(90 - 0) \tag{3}$$

where X_i is the load power for the first time period $(...)$;

(2) Output P_j of load power conservation unit $j(j = 1,2,3)$:

$$P_{j_i} = min_j + X_i(max_j - min_j) \tag{4}$$

Among them, min_j is the minimum technical output of the group j unit, and max_j is the maximum technical output of the group j unit.

(a) *Step 1: Calculate coal consumption per period*

The coal consumption per period F_i was calculated using the output of load power by the equation as follows:

$$F_i = a_j P_{ii}^2 + b_j P_{ij} + c_j \tag{5}$$

where a_j is the coal consumption parameter of the group j unit a,b_j is the coal consumption parameter of the group j unit b,c_j is the coal consumption parameter of the group j unit c, $P_{ij} = P_{ii}$.

(b) *Step 2: Build the combination and make the selection*

Construct possible combinations $Z_i = [1,2,...]$ for each time period, where the number represents the unit or sum of unit combination numbers, to calculate the unit output corresponding to the combination of unit output $Out_i = \sum S_{Z_i}$; S_{Z_i} represents the corresponding unit output under the elements of the current combination, and further coal is obtained Consumption F, under the premise that the unit output to meet the current demand, the combination with the smallest coal consumption is the plan formulated $Plan = [Plan_1, Plan_2, ..., Plan_{96}]$.

(c) *Step 3: Calculate the relevant parameters*

According to the plans formulated, the corresponding formula was used to obtain the results required for **Table 4**.

The following command was used in MATLAB**:**

for i = 1:96

Mei1(i) = a(1)*(P_1(i)²)+b(1)*P_1(i)+c(1); end

The technical output corresponding to unit 1 was obtained, the same goes for units 2, 3 and load requirements. The results are as follows:

Table 1. Parameter calculation values for each unit

Unit 1	Unit 2	Unit 3	Load requirements
355.05	177.53	88.76	375.11
359.33	179.66	89.83	384.28
367.20	183.60	91.80	401.14
361.81	180.90	90.45	389.59
359.62	179.81	89.91	384.91
355.52	177.76	88.88	376.11
355.05	177.53	88.76	375.11
352.27	176.14	88.07	369.16
349.94	174.97	87.48	364.15
354.77	177.38	88.9	374.50
348.99	174.49	87.5	362.12
348.15	174.08	87.4	360.33
345.06	172.53	86.7	353.71
347.91	173.95	86.8	359.81
346.04	173.02	86.1	355.81
…	…	…	…

Based on **Table 1**, the yield of each combination was calculated and then the best combination was selected by comparing whether the demand is met. The optimal combinations of corresponding yields are plotted into a curve, and the daily power generation planning curve is shown in **Figure 1.**
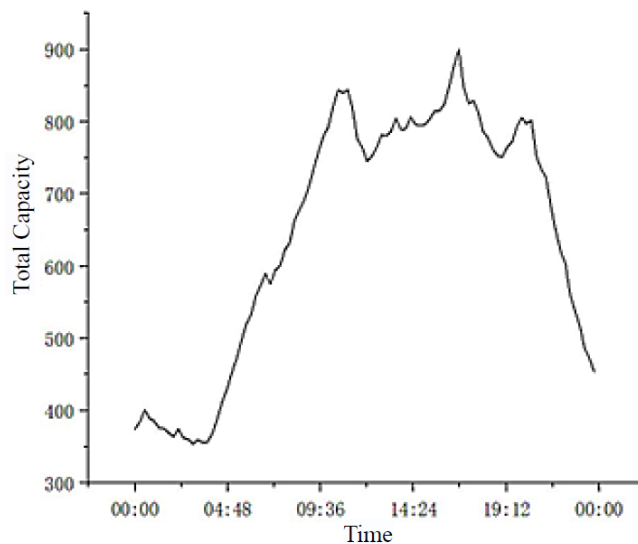
Figure 1. Daily power generation plan curve

Observing this curve, the sudden change occurred in the time period of 20 to 30 and the period of 90 to 96 in the middle of the curve, indicating that the power consumption is high Peak and night power demand is reduced.

The cost of solving the relevant parameters and analyzing the results is shown in **Figure 2**:
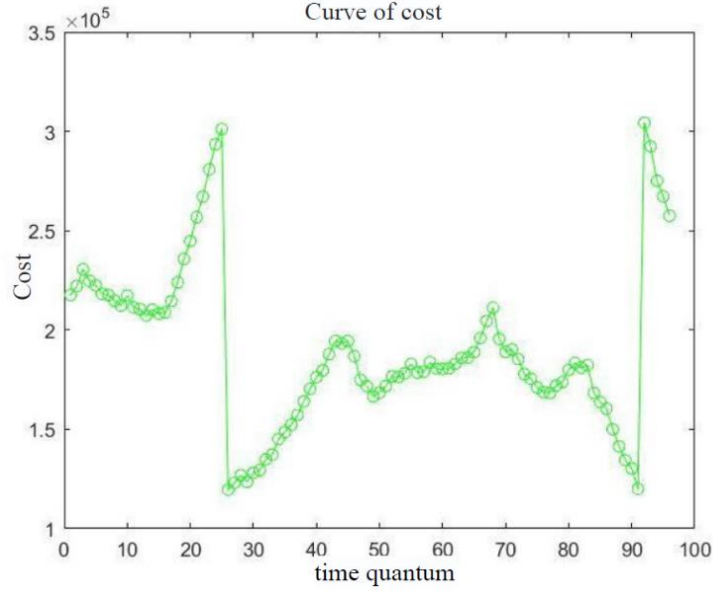
Figure 2. Cost curve

The parameters are calculated as follows (**Table 2**):

Table 2. Parameter calculation values for each part

Carbon capture book	Thermal power operating costs	Carbon capture book	Total cost of electricity generation	Unit power supply cost
0	2322.517	0	2322.517	72.33
60	2322.517	139.62	2468.27	91.25
80	2322.517	679.24	2889.62	103.28
100	2322.517	702.51	3592.57	112.76

5.2. Establishment of the model

(1) Step 1: Wind power conversion

First, the wind power was converted into the desired value, as follows: Convert the wind power into a wind turbine output

$$Fengdion_{base_i} = 0 + XX_i(B_j - 0) \tag{6}$$

Where XX_i is the wind power for the *i*th time period (i = 1,2, … ,96); B_j is the *j*th of the 300 iterations of wind power Installed capacity.

(2) Step 2: Iterate

The number of iterations was set to 300 times for the iteration of the curtailed wind and lost load, repectively.

$$\begin{cases} Qi_{feng_j} = \left(P1 + P2 + Fengdian_{base_j} * Qi_{log}\right) - 900 \\ Shi_{feng_j} = \left(P1 + P2 + Fengdian_{base_j} * Shi_{log}\right) - 900 \end{cases} \tag{7}$$

where Qi_{feng_j} is the curtail wind generated in the j iteration, Shi_{feng_j} is the loss generated in the j iteration. The Qi_{log} and Shi_{log} are logical judgment matrices.

(3) Step 3: Seek excellence

The relationship between sum of the values for wind curtailment, QS_{sum_i} and load loss for each iteration is expressed in the equation as follows:

$$QS_{sum_j} = \left| Qi_{feng_j} + Shi_{feng_j} \right|$$

The smallest QS_{sum_i} was identified, its corresponding installed capacity is the optimal installed capacity, corresponding to the curtailment and load loss is the best iterative field j corresponding to the Qi_{fena_i} and Shi_{fena_i}.

Problem 3 replaces the value of unit 2 with the same method. Problem 4 was calculated using the value directly on the basis of the first two questions, the relevant parameters were then calculated.

5.3. Solution and analysis of problem models
5.3.1. Problem 2 model solving and result analysis

In MATLAB, using the nested for loops, the outer loop was set to 300 iterations, the inner loop was set to 96 times to find the relevant parameters of 96 periods, and the results of the programming calculation are shown in **Table 3**.

Table 3. Abandon wind or loss of load

Optimal installed capacity	Abandon wind	Sum of the load losses
288	51153.50	2379.28
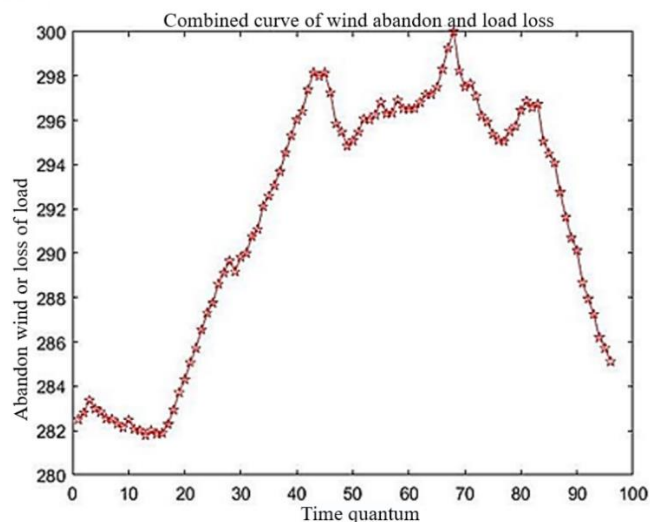
Figure 3. Wind and load loss curves

Looking at the figure above, the abscissa represents the 96 time periods from 00:00 to 23:45, and the ordinate is the corresponding curtailment or load loss, which reflects the system balance of each time period in a day (**Figure 3**).

5.3.2. Problem 3 model solving and result analysis

The programming calculation results are shown in **Table 4**.

Table 4. The results of the programming calculations

Optimal installed capacity	Abandon wind	Sum of the load losses
688	241153.50	20379.28

Draw the wind curtailment and load loss curves as follows:
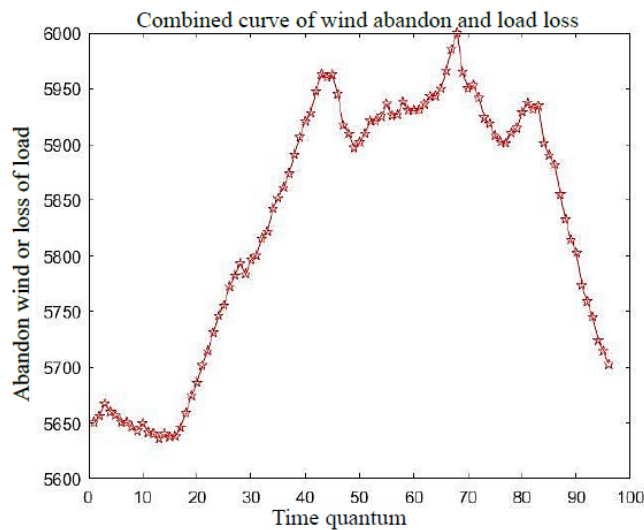
Figure 4. Wind curtailment and load loss curves

As shown in **Figure 4**, the abscissa represents the 96 time periods from 00:00 to 23:45, and the ordinate coordinate is the corresponding curtailed wind or loss The load size, with a maximum value of up to 6000, reflects the balance of the system over time of day (**Figure 5**).

5.3.3. Solution to Problem 4

When the installed wind power was replaced by 300WM and 600WM, the relevant indicators are shown in **Table 5** and **Table 6** below, respectively.

Table 5. Relevant indicators for wind power installed capacity when 300WM is replaced

Carbon capture	Thermal power operating costs	Carbon capture book	Wind power operation and maintenance costs	Wind loss		Loss of load loss		Unit power supply cost
				Discard wind power	Wind loss	Lost load power	Loss of load loss	
0	1683.27	581.27	291.35	45421	1892.56	40376	1682.35	821.2
60	1683.27	602.39	291.35	45421	1892.56	40376	1682.35	821.2
80	1683.27	688.27	291.35	45421	1892.56	40376	1682.35	821.2
100	1683.27	801.56	291.35	45421	1892.56	40376	1682.35	821.2

Table 6. Relevant indicators for wind power installed capacity when 600WM is replaced

Carbon capture	Thermal power operating costs	Carbon capture book	Wind power operation and maintenance costs	Wind loss		Loss of load loss		Unit power supply cost
				Discard wind power	Wind loss	Lost load power	Loss of load loss	
0	1783.58	481.28	381.75	35425	1292.56	39376	1582.35	973.6
60	1783.58	522.85	381.75	35425	1292.56	39376	1582.35	973.6
80	1783.58	588.97	381.75	35425	1292.56	39376	1582.35	973.6
100	1783.58	601.56	381.75	35425	1292.56	39376	1582.35	973.6

5.3.4. Establishment and solution of Problem 5 and Problem 6 models

(1) Establishment of the model

In response to Problem 5, the impact of wind power installed capacity of 900MW, replacement unit 2 and 3, the amount of lost load, the minimum energy storage capacity that needs to be configured (90% of the energy storage charging and discharging efficiency), and the energy storage cost on the grid frequency need to be considered.

VSWT internal losses and converter losses are negligible, and the active power P_g of its output is

$$P_g = P_m = \frac{1}{2}\rho\pi R^2 v_w^3 C_p(\lambda, \beta) \tag{8}$$

Based on equation (1), P_m is the mechanical power; R is the radius of the blade of the wind turbine; ρ for air density; v_w is the wind speed; $C_p(\lambda, \beta)$ is wind power. The wind energy utilization coefficient of the machine is a function of the blade tip speed ratio λ and the pitch angle β [1]:

$$C_p(\lambda, \beta) = 0.22(116\chi - 0.4\beta - 5.0)e^{-12.5\chi} \tag{9}$$

thereinto,

$$\chi = \frac{1}{\lambda + 0.08\beta} - \frac{0.035}{\beta^3 + 1}, \lambda = \omega_1 R/v_w \tag{10}$$

wherein: ω_r is the rotor speed; R is the blade radius of the wind turbine.

Under MPPT (Maximum Power Point Tracking) control, VSWT (Variable Speed Wind Turbines) operates at its maximum power point at either wind speed, and the maximum power constantly changes with wind speed, making the wind power random. Wind power forecasting can mitigate the impact of wind power randomness on the grid to some extent, but there is an error between the wind power forecast power and the actual value, known as WPPE. WPPE is prone to IUAP (Initial Unbalance of Active Power) of the power grid, which can be calculated by equation (11):

$$\Delta P_{L0} = \Delta P_{Load0} - \Delta P_W \tag{11}$$

At this time, the grid starts a frequency regulation, and the SG (Synchronous Generator) releases the rotor kinetic energy to smooth out the rapid changes in the grid frequency. However, a frequency

modulation is a differential adjustment, and the amount of change in the grid frequency from the initial value after a frequency regulation is called a static frequency deviation, which can be calculated using equation (12):

$$\Delta f_1 = -\frac{\Delta P_{L0}}{K_G + K_L} \cdot f_0 \tag{12}$$

Based on equation (5), K_G and K_L are the regulation coefficients of the grid equivalent SG and load, respectively; f_0 is the initial frequency of the grid.

The amount of power adjustment for the first I SG is:

$$\Delta P_{Gi}^I = -\frac{1}{R_i^*} \cdot \frac{\Delta f_1}{f_N} \cdot P_{Gi.0} \tag{13}$$

where $P_{Gi.0}$ is the initial active power of the first i SG; R_i^* is the standard value of the difference coefficient of the ith SG.

From equation (12) and (13), it can be seen that due to the large WPPE of the high-proportion wind power system, the static frequency deviation of the power grid after the primary frequency regulation is large, and the secondary frequency regulation of the power grid is started at this time. Secondary frequency regulation can usually achieve error-free regulation, but it is constrained by the frequency regulation capacity of the grid. In order to avoid frequency overruns, the FM (frequency modulation) capacity R_G required by the system should meet:

$$\Delta P_{L0} + (K_G + K_L)f_{lim}^- \le R_G \le \Delta P_{L0} + (K_G + K_L)f_{lim}^+ \tag{14}$$

Where f_{lim}^+ and f_{lim}^- are the upper and lower limits of the frequency fluctuations allowed by the grid.

It can be seen from the formula that in addition to load changes, the WPPE of the high-proportion wind power system makes the frequency regulation capacity required by the system larger, and the conventional SG standby plan according to the maximum power generation load configuration is difficult to meet the system frequency regulation requirements. The probability density curve of WPPE can be fitted with an improved generalized error distribution model, and its distribution interval can be estimated in combination with confidence, so as to appropriately increase the frequency modulation capacity of the system. Under a certain predicted wind speed, the distribution range of WPPE is usually from a certain negative value to a certain positive value, that is, IUAP can be positive or negative, so the grid should be equipped with sufficient positive and negative frequency modulation capacity at the same time.

The VSWT has fast and flexible power control capabilities, and by adjusting the rotor speed and pitch angle control reference values, it is able to move the operating point of the wind turbine so that it is in a load-reduced operation state. When IUAP occurs in the grid, the VSWT, which operates in advance, provides sufficient FM capacity for the grid. The load reduction operation is mainly aimed at the frequency deviation caused by the wind speed prediction error, which does not occur frequently. Besides, the safety constraints of the unit, the control stability, and mechanical performance of the VSWT can be guaranteed to the greatest extent through smooth control, so as to achieve rapid support for the grid frequency.

(2) Frequency control idea based on optimal load reduction of wind power

At a certain wind speed, the active power of VSWT increases; however, with the increase of rotational speed, the active power decreases. With MPPT control, the VSWTs operate at each of the maximum power points. Both OSC and PAC are able change the runtime point of VSWT to achieve load-shedding operation of VSWT. The OSC responds faster than the PAC, but when the rotor speed is ω_{max}, the rotor speed of the VSWT cannot be further increased, ω_{max} the OSC is only suitable for wind conditions with low to medium wind speeds. The PAC can achieve the load reduction operation of the VSWT at full wind speed, but because its control structure is a mechanical element, the response speed is slower, and frequent pitch changes are easy to cause wear of mechanical parts, which in turn increases the operation and maintenance cost of VSWT and reduces the service life of the wind turbine. Therefore, in order to reduce the load of the VSWT in the full wind speed range and reduce the wear of mechanical components such as wind turbines, when the rotor speed is lower than ω_{max} during normal operation, VSWT is preferred OSC implements load reduction; VSWT operates with a PAC when the rotor speed is ω_{max} during normal operation or when the rotor speed has been increased to ω_{max} via OSC. The maximum adjustment of pitch angle under PAC is limited by the pitch speed v_{β} and VSWT's FM time t_{ref}. Among them, t_{ref} is determined by the grid operation requirements, generally does not exceed the secondary frequency modulation response time of SG.

The VSWT load reduction control strategy is shown in **Figure 5**. Among them, V_{cr}, V_{w1} and V_n are the cut-in wind speed, the critical wind speed of the optimal speed zone and the rated wind speed, respectively. When the wind speed is v_w, under the action of OSC, the operating point of VSWT can move from point B along the curve BB′ to point B′, and when the operating point reaches B′, it is impossible to continue to use OSC to achieve load reduction. At this point, with the PAC, the operating point of the VSWT can be moved along the straight line B'F toward the F point. The F point is the operating point at a speed of ω_{max} and the pitch angle is the maximum adjustment amount $v_{\beta}t_{ref}$. Therefore, at any wind speed V_w, VSWT has a maximum reduceable load rate $d_{max}\%$, which can be expressed as

Figure 5. The load reduction control strategy for VSWT

$$d_{max}\% = \frac{P_{g.opt} - P_{de.max}}{P_{g.opt}} \tag{15}$$

thereinto,

$$\begin{cases} P_{de.max} = \frac{1}{2}\rho\pi R^2 v_w^3 C_p\left(\omega_{max}R/v_w, v_\beta t_{ref}\right) \\ P_{g.opt} = \frac{1}{2}\rho\pi R^2 v_w^3 C_P\left(\omega_{opt}R/v_w, 0\right) \end{cases} \tag{16}$$

where $P_{de.max}$ is the active power of the VSWT output at the maximum load reduction rate; $P_{g.opt}$ is the active power output of VSWT under normal operating conditions; ω_{opt} is the optimal speed of the rotor [2].

Under the operating state of load reduction, VSWT has positive and negative FM capacity, which is limited by $P_{g.opt}$ and $P_{de.max}$ respectively, and the negative FM capacity decreases accordingly as the positive FM capacity increases. As shown in **Figure 1**, VSWT operates at an optimal load reduction rate of must d_{opt} %. At point B$_0$, its maximum positive FM capacity ΔR_{up}^{max} and maximum negative FM capacity ΔR_{down}^{max} are respectively.

$$\begin{cases} \Delta R_{up}^{max} = P_{g.opt} - P_{de.opt} \\ \Delta R_{down}^{max} = P_{de.opt} - P_{de.max} \end{cases} \tag{17}$$

$P_{de.opt}$ is the active power of VSWT at the optimal load reduction rate.

$$P_{de.opt} = P_{g.opt}\left(1 - d_{opt}\%\right) \tag{18}$$

The FM capacity of SG and the FM capacity of VSWT together constitute the FM capacity of the grid. The required frequency regulation capacity of the power grid is related to WPPE, the probability distribution interval of WPPE under different confidence and wind speed is different, and the positive and negative frequency regulation capabilities of VSWT are interrelated. In addition, there is a certain economic loss in load reduction operation, and contrary to the SG start-up cost, the fixed load reduction rate cannot meet the needs of the grid. Therefore, the dynamic optimal reduction can be determined under the constraint of the maximum load loss rate according to the grid operating state, predicted wind speed and WPPE allocation interval load rate, taking into account the safety and economy of the power grid.

(3) Parameter conversion

The technical output generated by the thermal power unit 1 and 600MW wind turbines per period was calculated, and the total technical output *EE sum_* per period was converted using the equation as follows:

$$EE\_sum_i = P1_i + X_i * 600 \tag{19}$$

$$\begin{cases} EE\_chuneng_{ij} = EE\_sm_i, & if\ EE\_sm_i > 900, EE\_sm_i < Ron_j \\ EE_{shifuhe_{ij}} = EE_{sm_i}, & if\ EE_{sm_i} < 900 \end{cases} \tag{20}$$

$$delta = \|EE\_chuneng| - |EE\_shifuhe\| \tag{21}$$

Iteration minimizes the power difference, and then the number of outputs is the minimum energy storage capacity.

Problem 6 considers that it is impossible to have wind all the time, then directly set different wind turbine capacity on the basis of Problem 5, and then calculate the difference in electricity, the larger the difference, the more unstable the power supply, and then the relevant analysis of the calculation results can be performed.

(4) Model solving and results analysis

Programmed by MATLAB, the minimum energy storage capacity can be obtained for all values above 471. Considering that the larger the capacity, the more cost is required, so the minimum energy storage capacity is 471. The corresponding load loss capacity was calculated to be 2465.8. Consider the cost of energy storage, after capturing the cost per unit of carbon, the unit power supply cost of the system was 1026.87.

5.4. Establishment and solution of the problem seven model

5.4.1. Establishment of the model

For the fifteen-day load power (maximum 1200MW), wind power (installed capacity) shown in **Appendix 2** (Capacity 1200MW), replacing thermal power units 2 and 3 into wind power units, what are the problems in the system power balance? A possible power balance solution was designed and the feasibility and effectiveness of the solution will be discussed. The model that was built is shown as follows:

The standby mode of traditional generator sets is constrained by the formula (22) -(26).

$$P_{g,t}^0 + P_{g,t}^{0+} \leq P_g^{max} i_{g,t}, \forall g, t \tag{22}$$

$$P_{g,t}^0 - R_{g,t}^{0-} \geq P_g^{min} i_{g,t}, \forall g, t \tag{23}$$

$$R_{g,t}^{0+}, R_{g,t}^{0-} \geq 0, \forall g, t \tag{24}$$

$$P_{g,t}^0 + R_{g,t}^{0+} - P_{g,t-1}^0 + R_{g,t-1}^{0-} \leq R_{U,g}(1 - u_{g,t}) + P_g^{min} u_{g,t}, \forall g, t \tag{25}$$

$$P_{g,t-1}^0 + R_{g,t-1}^{0+} + R_{g,t}^{0-} - P_{g,t}^0 \leq R_{D,g}(1 - v_{g,t}) + P_g^{min} v_{g,t}, \forall g, t \tag{26}$$

where $R_{g,t}^{0+}$, $R_{g,t}^{0-}$ represent the up-and-down backup capacity provided by the traditional generator set under the pre-scheduling decision time scale, respectively. At the same time, it should be noted that in order to improve the fluency of the text and avoid the description of duplicate information, except for the introduction of new physical quantities or special instructions, the physical quantities used in the models mentioned later in this article are the same as those in **Part 2** of the paper, and no repeated interpretations are made.

Under the time scale of the rescheduling decision, the constraints of the traditional generator set output and standby capacity adjustment are shown in the formula (27) -(31).

$$P_{g,t}^u = P_{g,t}^0 + \Delta P_{g,t}^{u+} - \Delta P_{g,t}^{u-}, \forall g, t \tag{27}$$

$$0 \le \Delta P_{g,t}^{u+} \le R_{g,t}^{0+}, \forall g, t \tag{28}$$

$$0 \le \Delta P_{g,t}^{u-} \le R_{g,t}^{0-}, \forall g, t \tag{29}$$

$$R_{g,t}^{u+} = R_{g,t}^{0+} - \Delta P_{g,t}^{u+}, \forall g, t \tag{30}$$

$$R_{g,t}^{u-} = R_{g,t}^{0-} - \Delta P_{g,t}^{u-}, \forall g, t \tag{31}$$

In the formula, $\Delta P_{a.t}^{u+}$ and $\Delta P_{a.t}^{u-}$ indicate the up-and-down of the standby capacity of the traditional generator set invocation under the rescheduling decision time scale, respectively; $\Delta P_{a.t}^{u+}$ and $\Delta P_{a.t}^{u-}$, represent the remaining spare capacity after the power adjustment of the traditional generator set, respectively; that is, the backup capacity that can be provided under the time scale of the rescheduling decision to cope with other uncertainties such as random shutdown of power equipment. Since the rescheduling phase is closer to the actual operating conditions of the power system. As a result, the available standby capacity is smaller than during the pre-scheduling phase.

5.4.2. Standby modeling of wind farms

Similar to traditional generator sets, wind farms can provide backup for the system through active control. However, due to the uncertainty of wind power output, wind farm output and backup are greatly affected by the available wind power. When the actual available wind power in the remodeling phase is less than its forecast value, the wind farm will reduce its planned output, and the insufficient downsizing of reserve capacity will be reduced; When the actual available wind power is greater than the forecast value, the wind farm can increase its output to increase wind power consumption, and the power company will purchase more high-quality reserves to meet the adjustment demand. It should be noted that the reduction in the number of additional purchases for the downdraft also means a reduction in the shortage of regulated wind power.
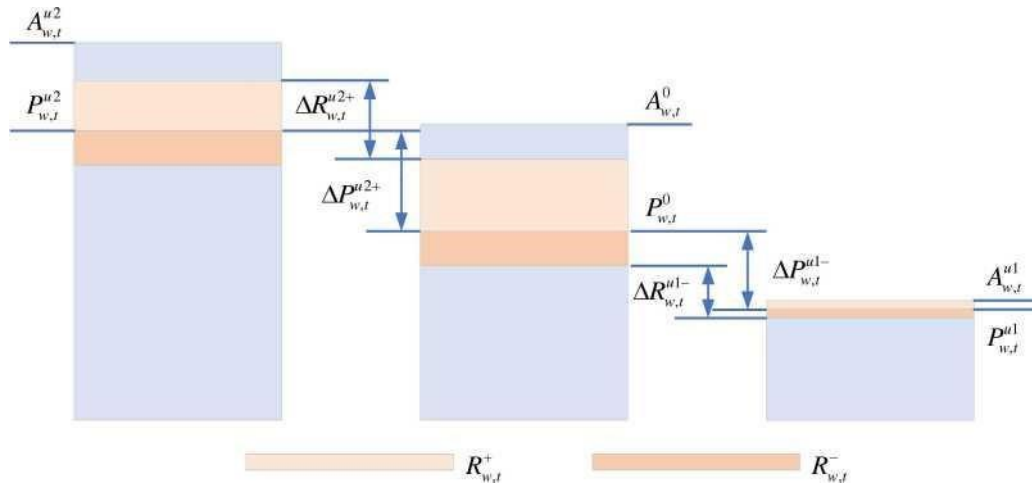
Figure 6. Wind farm output and backup methods

Figure 6 shows that the actual available wind power in the pre-scheduling decision stage and the rescheduling decision stage is less than the predicted value (superscript u1) and larger Schematic diagram of wind power output and backup method in the three scenarios of predicted value (superscript u2). Figured: For three scenarios, $R_{w,t}^+$ and $R_{w,t}^-$, both of which are up-and-down reserve capacity provided by the printed wind farm w, respectively; $\Delta P_{w,t}^+$ and $\Delta P_{w,t}^-$, respectively, are rescheduling decision scenarios The amount of adjustment of the upward and downward adjustment of the output of the lower wind farm relative to the pre-dispatch stage; $\Delta R_{w,t}^+$, and $\Delta R_{w,t}^-$, respectively, are additional purchases of the system to adjust and reduce the standby capacity during the rescheduling decision phase compared to the pre-scheduling phase [3].

Under the time scale of the pre-scheduling decision stage, the wind farm operation constraints are shown in the equation (32) - (33).

$$0 \leq R_{w,t}^{0+} \leq A_{w,t}^0 - P_{w,t}^0, \forall w, t \tag{32}$$

$$0 \leq R_{w,t}^{0-} \leq P_{w,t}^0, \forall w, t \tag{33}$$

$$P_{w,t}^u = P_{w,t}^0 + \Delta P_{w,t}^{u+} - \Delta P_{w,t}^{u-}, \forall w, t \tag{34}$$

$$0 \leq R_{w,t}^{u+} \leq A_{w,t}^u - P_{w,t}^u , \forall w, t \tag{35}$$

$$0 \leq R_{w,t}^{u-} \leq P_{w,t}^u, \forall w, t \tag{36}$$

$$\Delta P_{w,t}^{u+} \geq 0, \forall w, t \tag{37}$$

$$\Delta R_{w,t}^{u+} \geq \Delta P_{w,t}^{u+} - \Delta P_{w,t}^{u-} + R_{w,t}^{u+} - R_{w,t}^{0+}, \forall w, t \tag{38}$$

$$\Delta R_{w,t}^{u+} \geq 0, \forall w, t \tag{39}$$

$$0 \leq \Delta P_{w,t}^{u-} \leq R_{w,t}^{0-} + \Delta R_{w,t}^{u-}, \forall w, t \tag{40}$$

$$0 \leq \Delta R_{w,t}^{u-} \leq P_{w,t}^0 - R_{w,t}^{0-}, \forall w, t \tag{41}$$

$$R_{w,t}^{u-} = R_{w,t}^{0-} + \Delta R_{w,t}^{u-} - \Delta P_{w,t}^{u-}, \forall w, t \tag{42}$$

Equation (34) to (36) indicates that the standby retained by the wind farm during the rescheduling decision stage satisfies the same constraints as the pre-dispatch decision stage. Equations (37) to (39) and (40) to (42), respectively, describe the calculation process and numerical constraints of the redistribution of the redistribution on the wind farm in the decision-making stage shown in **Figure 6**.

5.4.3. Demand-side response modeling

This section models the mechanisms of action of the two demand-side response measures, PDR (price-based demand-side response) and IDR (incentive demand-side response).

(1) PDR (price-based demand-side response)

PDR adjusts the user's electricity consumption behavior by adjusting the time-sharing electricity price, and guides the user to reasonably transfer the electricity consumption period, so as to achieve the effect of peak shaving and valley filling. The power load after the implementation of PDR is shown in equation (44).

$$P_d = P_d^0 + \Delta P_d^{PDR} \tag{44}$$

where P_d^0 and ΔP_d^{PDR} represent the amount of load on node d before and after the PDR implementation, respectively; d is the load response after PDR implementation. The above three variables are in vector form and contain information about the moment being studied.

The correlation between load response and electricity price change is shown in equation (45).

$$\Delta P_{d,Nor}^{PDR} = E_d \cdot \Delta p_{d,Nor} \tag{45}$$

where $\Delta P_{d,Nor}^{PDR}$ and $\Delta p_{d,Nor}$ represent the normalized vector of node d load response and electricity price change, respectively; E_d is the elastic matrix of the electricity price of the node, and its self-elastic coefficient value indicates the user's response to the change of the electricity price in the current period, which is not positive [4]; The reciprocal elasticity coefficient value indicates the user's response to the change of electricity price in other periods, which is a non-negative value. $\Delta P_{d,Nor}^{PDR}$ and $\Delta p_{d,Nor}$ are in the specific forms, respectively, as shown in equations (46) and (47).

$$\Delta P_{d,Nor}^{PDR} = \left[\frac{\Delta P_{d,1}^{PDR}}{P_{d,1}^0} \frac{\Delta P_{d,2}^{PDR}}{P_{d,2}^0} \cdots \frac{\Delta P_{d,|T|}^{PDR}}{P_{d,|T|}^0} \right]^T \tag{46}$$

$$\Delta p_{d,Nor} = \left[\frac{\Delta p_{d,1}}{p_{d,1}^0} \frac{\Delta p_{d,2}}{p_{d,2}^0} \cdots \frac{\Delta p_{d,|T|}}{p_{d,|T|}^0} \right]^T \tag{47}$$

where: P_d^0 represents the benchmark value of the node d price, $|T|$ can be the number of hours studied. It should be noted that in order to avoid the sharp fluctuation of electricity prices in a short period of time, PDR is implemented in the pre-scheduling decision-making stage, and the electricity price obtained by the PDR is implemented before the rescheduling decision-making stage is maintained.

(2) IDR (incentive demand-side response)

Users participating in IDR are managed by load agents. The load agent integrates the response of the terminal load node and submits the compensation price to the power company for participating in the load reduction during the re-dispatching phase. Power companies make decisions on dispatch plans based on load reduction bidding and system operating conditions. For users participating in IDR, the utility company pays them not only the electricity compensation for the actual load reduction, but also the load reduction capacity fee. For the involuntary load shedding volume of users in the emergency operation scenario, the power company will pay a higher emergency load shedding fee. Compared to PDR, IDR is closer to a direct standby provider on the load side [5].

The IDR standby capacity determined during the prescheduling decision phase satisfies the constraint (48).

$$0 \leq P_{d,t}^{0,IDR} \leq P_{d,t}^{IDR,max}, \forall d,t \tag{48}$$

$$0 \leq \Delta P_{d,t}^{u,IDR} \leq P_{d,t}^{0,IDR}, \forall d,t \tag{49}$$

$$P_{d,t}^{u,IDR} = P_{d,t}^{0,IDR} - \Delta P_{d,t}^{u,IDR}, \forall d,t \tag{50}$$

where $\Delta P_{d,t}^{u,IDR}$ and $P_{d,t}^{u,IDR}$, represent the IDR standby capacity called during the rescheduling decision phase, and the standby capacity that can continue to be used on the demand side, respectively.

It should be noted that since the uncertainty interval of the load is relatively small relative to the total load, this chapter ignores the uncertainty of the demand-side response. However, if the situation needs to be considered, the treatment method of wind power can be used as a reference.

5.4.4. Stage model

(1) Objective function

The goal of the first phase of the RMRS model is to minimize the operating costs of the generator set and the cost of standby capacity for various standby resources, as shown in equation (51).

$$\min_{\Omega^0} C^0 = \sum_{t \in T} \sum_{g \in G} \left(\sum_{k \in K} C_g^k P_{g,t}^k + C_g^{nl} i_{g,t} + C_g^{su} u_{g,t} + C_g^{sd} v_{g,t} + C_g^{R+} R_{g,t}^{0+} + C_g^{R-} R_{g,t}^{0-} \right)$$
$$+ \sum_{t \in T} \sum_{w \in W} \left(C_w^{R+} R_{w,t}^{0+} + C_w^{R-} R_{w,t}^{0-} \right) + \sum_{t \in T} \sum_{d \in D} C_d^{IDR} P_{d,t}^{0,IDR} \tag{51}$$

where, C_w^{R+} and C_w^{R-} indicate the adjustment and reduction of spare capacity costs on the wind farm, respectively; $C_{d,t}^{IDR}$ is the capacity of the IDR.

(2) Generator set operation with standby constrains

The operation of traditional generator sets needs to meet the output segmented linearization constraint as shown in equations (52) and (53), start-stop constraint as shown in equations (54) to (57), and output, standby, and climb constraints as shown in equation (58).

$$P_{g,t}^0 = \sum_{k \in K} P_{g,t}^k \, , \quad \forall g, t \tag{52}$$

$$0 \le P_{g,t}^k \le P_{g,t}^{k,max}, \forall g, k, t \tag{53}$$

$$u_{g,t} - v_{g,t} = i_{g,t} - i_{g,t-1}, \forall g, t \tag{54}$$

$$u_{g,t} + v_{g,t} \le 1, \forall g, t \tag{55}$$

$$\left(X_{g,t-1}^{on} - T_g^{on}\right)\left(i_{g,t-1} - i_{g,t}\right) \ge 0, \forall g, t \tag{56}$$

$$\left(X_{g,t-1}^{off} - T_g^{off}\right)\left(i_{g,t} - i_{g,t-1}\right) \ge 0, \forall g, t \tag{57}$$

$$(52) - (56) \tag{58}$$

where $X_{a,t}^{on}$ and $X_{a\,t}^{off}$ table does not have generator set start-up time and downtime statistics, respectively. For the sake of the conciseness of the model description, this documents the adopted formula (56) - (57) describes the continuous start-up and downtime constraints of the generator set, and the specific unfolding type is as in the **Section 2** of the equation (19) and (20) shown.

(3) Wind farm output and standby constraints

Phase I constraints also include wind farm output and backup constraints (59).

$$(32) - (33) \tag{59}$$

(4) Demand-side response constraint PDR constraints are shown in equations (60) to (62), and IDR constraints are equations (63).

$$\Delta P_d^{PDR} = E_d \cdot \Delta p_d, \forall d \tag{60}$$

$$0 \leq \Delta P_{d,t}^{PDR} \leq \Delta P_{d,t}^{PDR,max}, \forall d, t \tag{61}$$

$$0 \leq \Delta p_{d,t} \leq \Delta p_{d,t}^{PDR,max}, \forall d, t \tag{62}$$

$$0 \leq P_{d,t}^{0,IDR} \leq P_{d,t}^{IDR,max}, \forall d, t \tag{63}$$

where $\Delta P_{d,t}^{PDR,max}$ and $\Delta p_{d,t}^{max}$ represents the maximum value of the load response and the change in electricity price, respectively, and the formula (61) and (62) are constrained the responsiveness of the PDR. The constraint (60) is a simplified form of equation (44) - (46), and the electricity price normalization information is contained in the elastic matrix Ed′.

(5) Power balance and transmission line power flow constraints

$$\sum_{g \in G_d} P_{g,t}^0 + \sum_{w \in W_d} P_{w,t}^0 + \sum_{l|to(l)=d} P_{l,t}^0 - \sum_{l|f,r(l)=d} P_{l,t}^0 = P_{d,t} + \Delta P_{d,t}^{PDR}, \forall d, t \tag{64}$$

$$-P_l^{max} \leq P_{l,t}^0 = \frac{\theta_{fr(l),t}^0 - \theta_{to(l),t}^0}{x_l} \leq P_l^{max}, \forall l, t \tag{65}$$

$$\underline{\theta} \leq \theta_{d,t}^0 \leq \overline{\theta}, \forall d, t \tag{66}$$

$$\theta_{ref,t} = 0, \forall t \tag{67}$$

Power balance and transmission line power flow constraints.

(6) Total standby capacity constraints

$$\sum_{g \subset G} R_{g,t}^{0+} + \sum_{w \subset W} R_{w,t}^{0+} + \sum_{d \subset D} P_{d,t}^{0,IDR} \geq R^{0,IDR}, \forall t \tag{68}$$

$$\sum_{g \in G} R_{g,t}^{0-} + \sum_{w \in D} R_{w,t}^{0-} \geq R^{0-,min}, \forall t \tag{69}$$

Wherein $R^{0+,min}$ and $R^{0-,min}$ represent the minimum value of the total spare capacity required to be adjusted up and down by the first stage of the system, respectively. Equation (68) indicates that the system up-and-down backup is provided by the traditional generator set, wind farm and IDR, while the

constraint (69) indicates that the system down-adjustment standby is provided by the generator set and the wind farm.

The optimization variables for the first phase of the RMRS model "Here-and-Now" decisions are included $i_{g,1}, u_{g,t}, v_{g,t}, P_{g,t}^0, P_{g,t}^k, R_{g,t}^{0+}, R_{g,t}^{0-} p_{w,t}^0, R_{w,t}^{0+}, \Delta P_{d,t}^{PDR}, \Delta P_{d,t}, P_{d,t}^{0,IDR}, P_{l,t}^0, \theta_{d,t}^0.$ Thereinto,

$P_{g,t}^0, P_{g,t}^k, R_{g,t}^{0+}, R_{g,t}^{0-}, p_{w,t}^0, R_{w,t}^{0+}, \Delta P_{d,t}^{PDR}, \Delta P_{d,t}, P_{d,t}^{0,IDR}, P_{l,t}^0, \theta_{d,t}^0$ should also be met, and the constraints of the second stage problem should also be met to ensure the safe and economic operation of the system under the actual wind power output conditions [7].

5.4.5. Uncertain set modeling

The RMRS model proposed in this chapter uses a box uncertainty set to characterize wind power output uncertainty, as shown in equations (70) - (71).

$$A_{w,t}^u = A_{w,t}^0 + Z_{w,t}^+ (A_{w,t}^{max} - A_{w,t}^0) - Z_{w,t}^- (A_{w,t}^0 - A_{w,t}^{min}), \forall w, t \tag{70}$$

$$0 \le Z_{w,t}^+, Z_{w,t}^- \le 1, \forall w, t \tag{71}$$

where $A_{w,t}^{max}$ and $A_{w,t}^{min}$ indicates the maximum and minimum values of the wind power output considered, respectively, and is a pre-set constant; $Z_{w,t}^+$ and $Z_{w,t}^-$ .It is used to characterize the degree of fluctuation of wind power output upward and downward, respectively, and the value is taken in between 0 and 1. When increased $A_{w,t}^{max}$ and $A_{w,t}^{min}$ The larger the uncertainty set of the RMRS model, the more robust the optimized scheduling plan, but at the same time the plan is more conservative; Conversely, the specified scheduling plan will be more economical and less reliable. Therefore, the system scheduling operator can adjust the size of the uncertain set according to its own preferences to achieve a balance between model economy and reliability.

It should be noted that in order to avoid the conservative nature of the model, the RMRS model only considers the uncertainty of wind and power output in the uncertainty concentration, while other multiple uncertainties such as load fluctuations and forced equipment shutdown have been taken into account in the total spare capacity constraint of the two-stage system. From this point of view, the value of $A_{w,t}^{max}$ and $A_{w,t}^{min}$ [8] can also be regarded as an uncertainty budget.

5.4.6. Second-stage model
(1) Objective function

The second phase of the RMRS model is an inner and outer layer problem. The inner layer problem is aimed at the possible actual wind power output, minimizing the adjustment cost of the output of the generating unit, the additional purchase cost of the wind farm standby, and other possible costs; The outer layer problem is not possible to determine the worst operating scenario. The objective function is shown in equation (72).

$$\max_U \min_{\Omega^u} C^u = \sum_{t \in T} \sum_{g \in G} (C_g^{uR+} \Delta P_{g,t}^{u+} + C_g^{uR-} \Delta P_{g,t}^{u-}) + \sum_{t \in T} \sum_{w \in W} [C_w^{uR+} \Delta R_{w,t}^{u+} + C_w^{uR-} \Delta R_{w,t}^{u-}$$

$$+ C_w^{cur}(A_{w,t}^u - P_{w,t}^u - R_{w,t}^{u+})] + \sum_{t \in T} \sum_{d \in D} (C_d^{u,IDR} \Delta P_{d,i}^{u,IDR} + C_d^{loss?} \Delta P_{d,t}^u) \tag{72}$$

Where: C_g^{uR+} and C_g^{uR-} indicate the output cost of the generator set up and down, respectively, where C_g^{uR+} is positive and C_g^{uR-} is negative. C_w^{uR+} and C_w^{uR-} are the costs of up-regulation and down-regulation of the reserve additional purchase of the wind farm; $C_d^{u,IDR}$ is the call cost of IDR standby capacity.

(2) Power balance and transmission line power flow constrains

$$\sum_{R \in d} P_{g,t}^u + \sum_{w \in W_d} P_{w,t}^u + \sum_{l|to(l)=d} P_{l,t}^u - \sum_{l|fr(l)=d} P_{l,t}^u$$

$$= P_{d,t} + \Delta P_{d,t}^{PDR} - \Delta P_{d,t}^{u,IDP} - \Delta P_{d,t}^u, \forall d, t \tag{73}$$

$$-P_l^{max} \leq P_{l,t}^u = (\theta_{fr(l),t}^u - \theta_{to(l)}^u)/x_l \leq P_l^{max}, \forall l, t \tag{74}$$

$$\underline{\theta} \leq \theta_{d,t}^u \leq \overline{\theta}, \forall d, t \tag{75}$$

(3) Alternate capacity calls with tuning constraints

The standby invocation and adjustment constraints for traditional generator sets, wind farms and IDR are shown in equations (76), (77) and (78), respectively.

$$(32) - (36) \tag{76}$$

$$(39) - (47) \tag{77}$$

$$(42) - (44) \tag{78}$$

(4) Emergency shear constraints

$$0 < \Delta P_{d.t}^u \leq P_{d.t} + \Delta P_{d.t}^{PDR}, \forall d, t \tag{79}$$

(5) Total standby capacity constraints

$$\sum_{g \in G} R_{g,t}^{u+} + \sum_{w \in W} R_{g,t}^{u+} + \sum_{d \in D} P_{d,t}^{u,IDR} \geq R^{u+,min}, \forall t \tag{80}$$

$$\sum_{g \in G} R_{g,t}^{u-} + \sum_{w \in D} R_{w,t}^{u-} \geq R^{u-,min}, \forall t \tag{81}$$

where $R^{u+,min}$ and $R^{u-,min}$ represent the minimum values of the total standby capacity required for the second stage system, respectively. The constraint in equations (80) and (81) means that after

adjusting the output of multiple resources according to the actual available wind power, the remaining spare capacity should still meet certain limits to cope with the uncertainty of the smaller time scale. Due to the shortening of the time scale, the load fluctuations faced by the system, and so on. The uncertainty factor is smaller, so the second phase standby capacity limit is lower than the first phase.

The optimization variables for the wait-and-see decision in the second phase of the RMRS model are included $P_{g,t}^u, P_{w,t}^u, \Delta P_{g,t}^{u+}, \Delta P_{g,t}^{u-}, \Delta P_{w,t}^{u+}, \Delta P_{w,t}^{u-}, \Delta P_{d,t}^{u,IDK}, \Delta P_{d,t}^u, P_{l,t}^u, \theta_{d,t}^u$ [9].

At the same time, in the actual scheduling operation process, the inner layer minimization model can be directly and independently solved according to the actual output of wind power to optimize the adjustment scheme of the system.

5.4.7. Compare model descriptions

To illustrate the effectiveness of demand-side response and wind farm backup, we will compare the scheduling results of whether to utilize these two standby resources in the study analysis section. For models that do not consider demand-side responses, the load response cap values can be set in Constraints (61) and (63) to 0. For models that do not consider the provision of backup for wind farms, the two-stage objective function can be modified to the form shown in equations (82) and (83), and the two-stage wind power output constraints are set to equations (84) and (85), respectively. It should be noted that the modified model can also be solved using the C&CG algorithm described in the following section [10].

$$
\min_{\Omega^0} C^0 = \sum_{t \in T} \sum_{g \in G} \left(\sum_{k \in K} C_g^k P_{g,t}^k + C_g^{nl} i_{g,t} + C_g^{su} u_{g,t} + C_g^{sd} v_{g,t} + C_g^{R+} R_g^{0+} + C_g^{R-} R_{g,t}^{0-} \right)
$$

$$
+ \sum_{t \in T} \sum_{d \in D} C_d^{IDR} P_{d,t}^{0,IDR}
$$

$$
\max_U \min_{\Omega^u} C^u = \sum_{t \in T} \sum_{g \in G} \left(C_g^{uR+} \Delta P_{g,t}^{u+} + C_g^{uR-} \Delta P_{g,t}^{u-} \right) + \sum_{t \in T} \sum_{w \in W} C_w^{cur} \left(A_{w,t}^u - P_{w,t}^u \right) \tag{82}
$$

$$
+ \sum_{t \in T} \sum_{d \in D} \left(C_d^{u,IDR} \Delta P_{d,t}^{u,IDR} \right.
$$

$$
+ C_d^{loss?} \Delta P_{d,t}^u \bigg) \tag{83}
$$

$$
0 \leq P_{w,t}^0 \leq A_{w,t}^0, \forall w, t \tag{84}
$$

$$
0 \leq P_{w,t}^u \leq A_{w,t}^u, \forall w, t \tag{85}
$$

Among the many flexible supply resources on the supply side, the power grid side and the demand side, the proportion of energy storage resources is small, and the demand side response resources are yet to form a fixed operation mode; various generator sets with strong stability and high reliability, including coal and gas, are an important part of meeting the variability and uncertainty on both sides of supply and demand.

6. Model advantages and disadvantages analysis

6.1. Advantages

(1) The single-objective optimization model can be applied in all the situations and provide an optimal solution;

(2) Multi-objective optimization can handle more complex optimization situations;

(3) Power systems can better cope with the uncertainty and volatility caused by the high proportion of wind power connected to the grid, thus ensuring the stable operation of the system in a more reliable and economical way.

6.2. Disadvantages

The robustness of the current model needs to be improved and can be optimized in conjunction with the DQN (deep-Q network) reinforcement learning method.

Disclosure statement

The author declares no conflict of interest.

References

[1] Sun W, Luo J, Zhang J, 2021, Analysis of Energy Storage Capacity Allocation and Influencing Factors of Power System with High Proportion of Wind Power Access. Power System Protection and Control 49(15): 9–18. https://www.doi.org/10.19783/j.cnki.pspc.201322

[2] Lu H, 2021, Research on Energy Storage Allocation Optimization and Comprehensive Value Measurement in New Power System, dissertation, North China Electric Power University (Beijing), 49(15): 9–18. https://www.doi.org/10.19783/j.cnki.pspc.201322.

[3] Yu H, Pan L, Wu Y, et al., 2020, Reliability Analysis of Energy Storage Improvement with High Proportion of Wind Power System. Power Grid and Clean Energy, 36(06): 92–98.

[4] Ren J, Xu Y, Dong S, 2018, Decentralized Dispatch Model of Interconnected Power System with High Proportion of Wind Power Considering Energy Storage Participation. Power Grid Technology, 42(04): 1079–1086. https://www.doi.org/10.13335/j.1000-3673.pst.2018.0012

[5] Li Y, 2020, Energy Storage Participates in the Study of Peak Regulation and Frequency Regulation of Power Systems Containing Wind Power, dissertation, Xinjiang University.

[6] Han S, 2018, Research on Optimal Allocation of Energy Storage in Power System with Large-Scale Wind Power, dissertation, Lanzhou Jiaotong University.

[7] Jiang Y, 2018, Research on the Active Dispatch Strategy of Energy Storage Participation in Power System under Large-scale Wind Power Access, dissertation, Southeast University.

[8] Han Y, Zheng X, Peng S, et al., 2015, Large-Scale Wind Power Centralized Access to the Power System Energy Storage Capacity Allocation Positioning Strategy, China Electric Power, 48(06): 26–31.

[9] Hou T, 2014, Research on Optimal Configuration of Energy Storage Power Supply in Power System with Large-Scale Wind Power, dissertation, Huazhong University of Science and Technology.

[10] Wu Y, 2018, Research on the Optimal Operation of Energy Storage Based on Reliability Assessment on the Participation of High Proportion of Wind Power Grid-Connected, dissertation, Changsha University of Technology Learning.

Appendix

21:45:00	0.721207	0.081183
22:00:00	0.690066	0.082807
22:15:00	0.671021	0.057448
22:30:00	0.6226	0.027733
22:45:00	0.598012	1.70E-05
23:00:00	0.574842	0.020574
23:15:00	0.540179	0.009199
23:30:00	0.52415	0.007064
23:45:00	0.503915	0.110092

Appendix 1

Date	Time	Load Power(MW)	Wind Power(MW)		
2020/7/1	0:00:00	577.771	1097.326		
2020/7/1	0:15:00	559.792	1092.743		
2020/7/1	0:30:00	563.602	1068.908		
2020/7/1	0:45:00	555.344	1022.154		
2020/7/1	1:00:00	538.012	1081.742		
2020/7/1	1:15:00	532.871	1003.82		
2020/7/1	1:30:00	530.356	981.818		
2020/7/1	1:45:00	524.362	894.729		
2020/7/1	2:00:00	524.104	931.398		

Appendix 2